

2700  
500  
NTIS

To be published in  
IEEE Trans. on Nucl. Sci.

BNL 19488

Presented at 1974 Nuclear Science  
Symposium & 14th Scintillation &  
Semiconductor Counter Symposium,  
Washington, D. C., Dec. 11-13, 1974.

CONF-741213--10  
CONF-741212--10

**FAST NEUTRON RADIATION DAMAGE OF  
HIGH-PURITY GERMANIUM DETECTORS\***

H. W. Kraner

Brookhaven National Laboratory  
Upton, New York 11973

and

Richard H. Pehl and Eugene E. Haller

Lawrence Berkeley Laboratory  
Berkeley, California 94720

**MASTER**

December 1974

The Energy Research and Development Administration (ERDA) is the successor to the U.S. Atomic Energy Commission (AEC) and all references to the AEC herein shall be deemed to refer to ERDA

\*This work was performed under the auspices of the  
U. S. Atomic Energy Commission.

DISTRIBUTION OF THIS DOCUMENT UNLIMITED

To be published in  
IEEE Trans. on Nucl. Sci.

BNL 19488

Presented at 1974 Nuclear Science  
Symposium & 14th Scintillation &  
Semiconductor Counter Symposium,  
Washington, D. C., Dec. 11-13, 1974.

FAST NEUTRON RADIATION DAMAGE OF  
HIGH-PURITY GERMANIUM DETECTORS\*

H. W. Kraner

Brookhaven National Laboratory  
Upton, New York 11973

and

Richard H. Pehl and Eugene E. Haller

Lawrence Berkeley Laboratory  
Berkeley, California 94720

December 1974

**NOTICE**  
This report was prepared as an account of work sponsored by the United States Government. Neither the United States nor the United States Energy Research and Development Administration, nor any of their employees, nor any of their contractors, subcontractors, or their employees, makes any warranty, express or implied, or assumes any legal liability or responsibility for the accuracy, completeness or usefulness of any information, apparatus, product or process disclosed, or represents that its use would not infringe privately owned rights.

\* This work was performed under the auspices of the U. S. Atomic Energy Commission.

**MASTER**

204

FAST NEUTRON RADIATION DAMAGE OF  
HIGH-PURITY GERMANIUM DETECTORS\*

H. W. Kraner  
Brookhaven National Laboratory  
Upton, New York 11973

and

Richard H. Pehl and Eugene E. Haller  
Lawrence Berkeley Laboratory  
Berkeley, California 94720

ABSTRACT

Seven high resolution, high-purity planar germanium and two lithium-drifted germanium detectors have been exposed to fluences of monoenergetic fast neutrons of 1.4, 5.5 and 16.4 MeV to study radiation damage effects. Seven of the exposures were made at 5.5 MeV using detectors made from both LBL and General Electric Company material. Initial degradation of  $^{60}\text{Co}$  energy resolution was generally observed after fluences of  $3 \times 10^{19}$  n/cm<sup>2</sup>. After fluences of  $10^{20}$  n/cm<sup>2</sup>, the detector resolutions were all affected, and replacement would be required in most gamma ray spectrometry; these results are consistent with previous damage studies on germanium detectors. Considerable variability in neutron damage threshold between detectors was observed within this fluence range which must be attributable to a material parameter that is not yet fully determined. This is the major finding in this study.

After irradiation, a significant increase in material resistivity was observed as a series resistance in the diodes undepleted region at low biases. The observations were made by capacitance effects and lengthened pulse rise time.

Annealing of damage was observed during storage at LN<sub>2</sub> temperature after irradiation; resulting, in some cases, in improvement of resolution and in others, further degradation. Drastic resolution degradation was observed on cycling detectors to dry ice temperatures, (200° K) with the loss of the high series resistance and an increase in acceptor concentration. Further cycling to room temperature for periods of hours resulted in improvement of the energy resolution compared with the 200° K value. Nearly complete recovery of initial charge collection and energy resolution was achieved by 100° C anneals for periods of hours indicating the possibility of in situ anneals.

No difference was found for the fast neutron damage susceptibility between planar high-purity and lithium-drifted germanium detectors.

Introduction

Several studies of the radiation damage effects of fast neutrons on germanium spectrometers have developed a great deal of empirical information<sup>1,2,3,4</sup>. Both Ge(Li) and high-purity germanium detectors have been studied; observable degradation of spectrometer

performance is generally similar, but no direct comparison has been made prior to this report.

The individual and specific observable damage result in a given detector is not particularly different in this study from those previously reported. Tailing and resolution degradation occurs due primarily to hole trapping and the detector performance can be recovered by a certain temperature anneal. This study was undertaken to address several outstanding questions:

- (1) What is the best estimate of the neutron fluence for "threshold" of damage in high quality gamma-ray spectrometers? Units to be studied should possess a full width at half maximum energy resolution of the 1332 keV  $^{60}\text{Co}$   $\gamma$ -ray of  $\leq 2$  keV and be at least 1 cm in thickness in a planar geometry.
- (2) What is the variability or range of this threshold in spectrometers made from different crystals of high purity germanium. Three detectors made from General Electric Co. material and four detectors made from LBL material were used. In addition, two Ge(Li) detectors made from LBL material were exposed.
- (3) What can we learn about relatively low temperature annealing of damage even to the extent of allowing in situ anneals of spectrometers. (100° C would be a practical value to aim for.)

Unfortunately, little physical interpretation of the electronic effects can be given in terms of microscopic detail due to the limited knowledge of the dynamics of collision produced vacancies and their coagulation and recombination. The details of the vacancy production mechanisms are to be found in the literature of charged particle interactions<sup>5</sup> and are generally better understood. Fast neutrons ( $E = 5$  MeV, for example) produce germanium atom recoils primarily by elastic scattering wherein the recoil atom receives at most 4/73 of the neutron energy which results in a 280 keV Ge ion recoil and a vacancy. Other reactions such as (n, $\alpha$ ) and (n,T) account for relatively little energy loss<sup>1,6</sup>. The Ge ion suffers both ionizing and

\* This work was performed under the auspices of the U. S. Atomic Energy Commission.

direct nuclear (vacancy producing) collision is slowing down with  $\sim 200^2$ . The ratio between the fractional energy loss in ionizing and nuclear collisions has been computed by Lindhard<sup>7</sup> and it is shown that the fraction of energy loss to nuclear collisions increases as the ion slows down until it dominates the energy loss process below  $\sim 200$  keV<sup>8</sup>. More vacancies are therefore produced by secondary collisions of neutron-produced germanium ions as they approach the end of their range. It can be remarked, then, that the proportionality of damage effect (or number of vacancies per neutron) to fast neutron energy is mitigated by this "end-of-range" non-linearity. This situation has been observed<sup>1</sup> and helped to de-emphasize the need to include fast neutron energy as a parameter in this study. Primarily, then, to concentrate the effort, most irradiations were performed at a single, intermediate energy, approximately 5.5 MeV.

#### Experimental Arrangement

Fast neutrons were obtained using several well known low energy reactions at the Brookhaven 5.5 MV Electrostatic Research Accelerator. One detector was exposed to 1.4 MeV neutrons using the  ${}^7\text{Li}(p,n){}^7\text{Be}$  reaction from a  $\sim 1$  mg/cm<sup>2</sup> LiF target. Another detector was exposed to 16.4 MeV neutrons from the  $\text{D}(T,n){}^4\text{He}$  reaction with a 1 MeV deuteron bombardment of a  $\sim 2$  mg/cm<sup>2</sup> tritiated titanium target. All other detectors were exposed to 5.5 MeV neutrons from the  $\text{D}(D,n){}^3\text{He}$  reaction; one using a 1 mg/cm<sup>2</sup> deuterated titanium target and four using a much thicker 6 mb/cm<sup>2</sup> target. As is indicated, all targets were not strictly "thin" and thus did not produce highly monoenergetic neutrons; the energies quoted for each neutron energy are the maximum energy with spreads downwards of at most 300 keV. All targets were deposited on flattened copper tubing through which a thin sheath of cooling water flowed.

Flux measurements were made with a Harwell-type long counter<sup>9</sup> placed approximately 1 meter from the target at about  $20^\circ \pm 8^\circ$  from the forward direction. The detectors to be exposed were placed at lesser distances ( $\sim 10$  cm) to increase the available flux and also at  $20^\circ \pm 8^\circ$  to the beam direction in the adjacent quadrant; errors caused by an angular distribution are thus minimized. The experimental area is floored with an iron grating and is physically a large open area which minimizes scattering and the possibly large uncertainties in flux determination. The active center of the long counter was found to  $12 \pm 2$  cm from the face at all energies used. Absolute flux calibration was made by comparison with a standard PuBe source of  $9.5 \times 10^5$  n/sec. Because the PuBe neutron spectrum is centered at approximately 5 MeV, no correction for relative long counter efficiency is made to the standardization at 5.5 MeV. The long counter efficiency<sup>9</sup> is greater in the 1-2 MeV range by only a few percent than that at 5 MeV and no correction was made to flux measurements for the 1.4 MeV run. However, a drop of efficiency of approximately 12% at 16.4 MeV compared to 5 MeV is noted, which was applied to the flux measurement at 16.4 MeV. Due to scattering, possible relative efficiency anomalies of the particular long counter and positioning uncertainty, errors of at least 25% must be assigned to these flux measurements. Count rate effects due to dead time losses were found to be unimportant.

Because most of the detectors exposed used cooled F.E.T. first amplification stages within the cryostat and both detector terminals were not available, de-

detector capacitance could not be measured directly with standard techniques, such as a bridge. The capacity was determined as a function of detector bias after each neutron exposure by inserting a square-wave pulse of known amplitude through the detector from the high voltage bias input and observing the induced charge relative to that of a known  $\gamma$ -ray. This method presumes that the detector is a network dominated by only the depleted volume capacitance and that other elements such as series resistances are minimal. Further remarks on this method will be made. Series resistances were, in fact, observed which affected this measurement and also the preamplifier output pulse shapes, the oscillographs of which were photographed. Detector leakage currents were monitored as the voltage across the preamplifier feedback resistor.

Spectra of  ${}^{60}\text{Co}$  and a calibration pulse were accumulated after each exposure to monitor the energy resolution degradation. The 1332 keV (upper)  ${}^{60}\text{Co}$  line is used to describe the detector resolution; the detector contribution is distinguished from the system (pulsar) resolution. A standard NBS disc  ${}^{60}\text{Co}$  source was placed on the detector cap in an effort to achieve reproducible relative efficiency data over the course of the total exposure. For the runs at 5.5 and 16.4 MeV, a lead brick had to be inserted between the target and the detector to reduce the large activation backgrounds seen in the target.

#### Neutron Damage Threshold

Approximately 10 min runs on  ${}^{60}\text{Co}$  were made after each exposure; the 1332 keV line was observed together with the pulsar inserted through the high voltage bias of the detector. The detector response was found to both broaden in FWHM and become "tailed" as carrier trapping became preponderant as previously observed<sup>1,2,3,4</sup>. Resolution effects are reported for the same detector bias used in the preirradiated condition and using the initial energy dispersion derived from the energy difference of the two  ${}^{60}\text{Co}$  lines at 1173 and 1332 keV. The tailing is only reported descriptively.

After damage, detector No. 215-6.0, irradiated at 1.4 MeV, was scanned with a collimated  ${}^{241}\text{Am}$  source to determine the carrier type predominantly trapped. The relative pulse height of the 60 keV  $\gamma$ -ray between source directed near the Pd(p<sup>+</sup>) contact compared with the source incident near the Li(n<sup>+</sup>) contact showed predominant hole trapping as has been abundantly demonstrated<sup>1,2,3,4</sup>.

Fig. 1 is a cable-graph which attempts to summarize the damage threshold results for the nine detectors irradiated. The boxes are measurements after the indicated fluence. Their widths correspond to the  $\pm 25\%$  estimated uncertainty in flux dot termination. Lower numbers in boxes are measurements made after the number of hours indicated in the parenthesis. All detectors were run at biases which assured full depletion or some over voltage. In some cases the detector was able to take more bias as irradiation proceeded and that increase improved resolutions; that result is also indicated in the lower part of the box.

All detectors except GEL were nominally 10 mm thick. GEL was 6 mm thick and might therefore be expected to be apparently somewhat more radiation resistant due to the shorter carrier transit.

Radiation damage "threshold" may be defined opera-

tionally to embrace both the fast neutron fluence for which the detector  $\gamma$ -ray energy resolution is noticeably worsened and that value for which the energy resolution is so worsened to strongly suggest replacement. These considerations imply an energy resolution degradation to about 3 keV (FWHM) for a typical gamma-ray spectrometer. There are other applications, specifically in the use as charged particle detectors, in which replacement would not be required at this resolution, but for sake of a number, we will use 3 keV.

Several initial conclusions may be drawn from the data of Fig. 1:

- (1) First of all: a range of thresholds from  $10^9$  n/cm<sup>2</sup> to  $10^{10}$  n/cm<sup>2</sup> is evident for the exposures at 5.5 MeV. Considerable difference is observed between and among the high-purity and Li-drifted units. It is apparent that there exist one or more material parameters which can characterize radiation damage sensitivity. This parameter(s) is not yet determined.
- (2) A dependence of damage threshold on neutron energy is not strongly evident from the comparison of detectors exposed at 1.4 and 16.4 MeV with those exposed to 5.5 MeV neutrons. Detector 214-6.0 (1.4 MeV) was not significantly longer lived than several units exposed at 5.5 MeV, although the very low bias (300V) tolerated by this detector may have somewhat reduced its observable threshold. In comparison, the threshold of 285-1.0 (16.4 MeV) was no doubt extended by its high bias condition of 2000V. Detector 265-1.0 (16.4 MeV) was, however, not significantly more damage sensitive than several exposed at 5.5 MeV, 284-1.2 for example.
- (3) The thresholds for Li-drifted detectors lie in the range between  $10^9$  and  $10^{10}$  n/cm<sup>2</sup> and are not different from high purity material. Although this threshold is somewhat less than that reported years ago we caution again that these are both high resolution and thick (10 mm) detectors with, therefore, a much greater sensitivity to resolution degradation.
- (4) The response may be grouped into two categories:
  - (a) low damage threshold - LBL Nos. 284-1.2 and 287-1.1 and
  - (b) higher damage thresholds - LBL No. 214-6.0 and the three detectors from two samples of GE material.

Attempts to find some common parameter within this grouping will be discussed.

- (5) Differences were noted between detectors in the apparent annealing at L<sub>2</sub> temperature immediately following damage and after several hours of storage, typically overnight. Noticeable worsening of energy resolution occurred to GE2 40 hours after  $7 \times 10^9$  n/cm<sup>2</sup> as the resolution went from 5.3 keV to 11.6 keV. This effect was also observed on GE3 and GE1. The slight im-

provement to 285-1.0 eleven hours after  $6 \times 10^9$  n/cm<sup>2</sup> may be due to an overall reduction in count rate as activation products in the system itself decayed. An improvement with time is noted for 214-6.0 and 287-1.1. It must be cautioned that this effect is especially noticeable after real damage has occurred. Some changes in the peak shape from broadening to events further displaced into a tail were noticed. In this case it is not totally descriptive to characterize the peak by just the FWHM. This is also the case in the apparent improvement of GE2 immediately following irradiation of  $1 \times 10^{10}$  n/cm<sup>2</sup> compared with 40 hours after  $7 \times 10^9$  n/cm<sup>2</sup>.

- (6) Following irradiations, more bias may be applied to the detector; somewhat more may be required for depletion. Increased bias did improve the degraded resolution, however in all cases noticeable improvement was obtained after severe degradation had occurred. Some extension of the useful detector lifetime can thus be achieved, which could be especially useful in charged particle applications involving complicated systems such as proton telescopes.

#### Capacitance and Series Resistance

The application of a voltage pulse into the high voltage or bias side of the detector is a convenient and accurate means of measuring the detector capacity. It is the only convenient means when using an internal FET first amplifier stage. However, when a significant series resistance through the detector is present the preamplifier output pulse shape is modified from the normal capacitive-coupled step function response and the depleted detector capacity can not be ascertained by this technique. Indeed Haller<sup>10</sup> et al have used this effect to study the material resistivity changes at very low temperatures. Fig. 2 shows the equivalent RC circuit of the detector with undepleted region having parameters  $R_0$  and  $C_0$ .  $C_d$  is the depleted region capacity and the boundary condition is that the geometrical capacity of the units  $C_0$  is  $C_0 C_d / (C_0 + C_d)$ . The preamplifier output voltage is essentially  $Q(t)/C_f$  in a charge sensitive amplifier;  $C_f$  is the feedback capacitor in the operational loop. For a voltage step function applied to the undepleted side of the detector, it has been shown that the preamplifier output voltage is

$$\frac{C_d}{C_f} \left[ 1 - \frac{C_d}{C_0 + C_d} \exp \left( - \frac{t}{R_0(C_0 + C_d)} \right) \right]$$

This response is described asymptotically as an initial quick rise to  $C_0/C_f$ , followed by a further slow rise to  $C_d/C_f$  with the time constant  $R_0(C_0 + C_d)$ . We note that a significant value of  $R_0$  will introduce  $C_0$  into the capacitive component of the impedance and cause the capacity to approach the geometrical value of  $C_0$ .

Figs. 3, 4, and 5 illustrate the change in apparent detector capacity at several fluences on detectors 284-1.2, 1098-4 and 287-1.1. The capacity does approach and reach the geometrical value after considerable irradiation. We note also that in the early stages of irradiation, the detector capacity as a function of a bias tends to be very slightly higher than the pre-irradiation values. These C(V) measurements are made directly after the irradiation and may represent the initial effect of free vacancies. Figs. 6, 7 and 8 are oscillographs of the preamplifier output waveforms

of the detector described by C(V) above, 284-1,2, 1098-4 and 287-1,1. In Figs. 7 and 8 we see the increase in the series resistance as the neutron exposure proceeded for detectors held at a particular bias.

Fig. 6 illustrates the change in relative final fraction ( $C_d/C_f$ ) to the initial step  $C_0/C_f$ . The pulse shape described by the formula has been well fitted to the observed shape at 10V bias with a time constant,  $R_d(C_0+C_d)$ , of 1.0  $\mu$ sec. An additional factor,  $e^{-t/\tau}$ , was included to account for the preamplifier clipping time of  $\approx 9.4$   $\mu$ sec. Using the voltage-depletion depth relationships, a time constant of 0.57  $\mu$ sec is derived for the 30V bias condition and a reasonable fit to this observed pulse shape was also obtained. These values of  $\tau$  allow the calculation of a bulk resistivity of 120K $\Omega$ -cm for this particular irradiation condition and material. Because of the complicated nature of the defect levels, both in number and in position in the gap, the next step in estimating the position of the Fermi level is not attempted. It is also anticipated that the irradiation may affect the carrier mobilities and further complicate the relationship of the resistivity to the number of defects.

At very high values of  $R_d$  with the apparent capacity at  $C_0$ , the output waveform is once again fast rising directly to the value  $C_0/C_f$ ; the very long time component is now much longer than preamplifier and main amplifier clipping times. The bottom oscillograph of Fig. 8 illustrates this waveform which in observable shape is not unlike the preirradiation waveform. (In this series, there was no relative normalization of the pulser relative to a  $^{137}\text{Cs}$  source also included during the measurement.) The output waveform at this stage of irradiation may indeed be confused with the initial preirradiation waveform, except for its amplitude.

#### Annealing

When a high-purity germanium spectrometer has been radiation damaged to the point it no longer is deemed useful, one is faced with the question - can the detector be easily repaired? Although little basic physical knowledge of the recovery processes is clearly understood, we can answer the practical question affirmatively. To illustrate the general annealing behavior, data on several detectors will be presented. Their history is fairly typical although differences between individual detectors do exist.

The spectrometer performance of detector 214-6.0 as a function of annealing treatment is outlined in Fig. 9(a) and 9(b) where the shape of the 1332 keV  $^{60}\text{Co}$  line at various stages is presented. The peaks have been displaced and the energy scale varied for clarity of illustration; peak position is not relevant.

Stage 1. This represents the situation prior to neutron irradiation. Detector 214-6.0 ranks as one of the best ever achieved at LBL. It was fabricated from a wafer cut from crystal #214 at a position where the net impurity concentration was only  $2 \times 10^9$  donors/cm $^3$ . As shown in Fig. 10, depletion was reached around 100V; the bend in the C-V relationship probably arises because this material had a p-type periphery.

The application of only 350V on this 1 cm thick detector resulted in excellent spectrometer performance; a nearly perfectly symmetrical 1.8 keV (FWHM) peak from the 1332 keV  $^{60}\text{Co}$  line. All spectra presented in Figs. 9(a) and 9(b) were obtained at 1000V.

Stage 2. After being irradiated by a fluence of  $10^{10}$  n/cm $^2$  1.4 MeV neutrons, the detector had remained at its normal operating temperature, a few degrees above LN $_2$ , for 7 days before these measurements were made. This detector appears to improve slightly during LN $_2$  anneal. However, this is not a characteristic of all neutron irradiated detectors. As noted in Fig. 1 some detectors deteriorated significantly during LN $_2$  anneal.

Stage 3. This represents the situation after the detector had been annealed at dry ice temperature for 15 h. The material is now p-type, and depletion is not reached until 1400V. A substantial increase in acceptor concentration was observed for all the detectors irradiated; similar observations have been reported previously $^{2,3}$ . A scan with collimated  $^{241}\text{Am}$  60 keV  $\gamma$ -rays from contact to contact revealed severe hole trapping. The severe degradation caused by the relatively cold anneal serves as a warning against warming any high-purity germanium detector that has been in significant neutron flux even if that detector has not shown any degradation. Bitter experience has dramatically proven this point. Several excellent one cm thick detectors (1.8 keV FWHM at 1332 keV) that have been used around accelerators at LBL without exhibiting measurable degradations have been warmed to room temperature for brief periods. Spectrometers with resolutions of 3 keV at 1332 keV were the result.

Stage 4. At this point the detector has been annealed at dry ice temperature an additional 32 h (total of 47 h). Depletion is now reached at 1050V, thus the acceptor concentration is already decreasing. Although still very poor, the  $^{60}\text{Co}$  spectrum has improved considerably relative to Stage 3.

Stage 5. An additional 82 h at dry ice temperature produced negligible change in either the spectrometer performance or acceptor concentration.

Stage 6. The detector had been annealed at room temperature for 14 h. Although the spectrometer performance improved somewhat the acceptor concentration was not measurably lower.

Stage 7. An additional 64 h at room temperature had now transpired. The spectrometer performance is considerably improved and depletion is now reached at about 980V.

Stage 8. The detector system was transported warm from BNL to LBL, and an additional 8 days at room temperature had elapsed. This lengthy room temperature anneal produced negligible change in either the spectrometer performance or acceptor concentration.

Stage 9. The detector was annealed 100 $^\circ\text{C}$  for 4 h prior to these measurements. Marked improvement in spectrometer performance is observed and depletion is now reached at about 850V. For many applications this detector would now be considered acceptable, especially if significant overvoltage could be applied.

Stage 10. An additional 102 h of annealing at 100 $^\circ\text{C}$  had now transpired. The detector is now acceptable for nearly all application although the spectrometer performance is not yet equal to the initial quality. As expected, the degradation relative to initial conditions is seen especially at lower bias, and when one looks carefully at peak symmetry. However, if a comparison is made when 2500V are applied,

little, if any, difference can be seen. Depletion is now reached at about 600V.

Stage 11. The detector was stored at room temperature for 192 h. Neither the spectrometer performance nor the acceptor concentration was affected measurably.

Stage 12. The detector was stored at room temperature for an additional 134 days. Although the depletion voltage has decreased to about 500V the spectrometer performance has remained essentially the same.

While stored at room temperature following sufficient 100°C annealing to largely restore spectrometer performance, the acceptor concentration decreased in all the detectors.

From these data one can conclude that in situ annealing of high-purity germanium spectrometers is possible. Although complete recovery may not be obtainable with 100°C annealing the spectrometer performance should be acceptable for nearly all applications. As an illustration of what can be done in the field the following case history is presented<sup>11</sup>.

During the testing of a high-purity germanium detector system at the Los Alamos Meson Physics Facility (LAMPF) it was exposed to a total neutron dose of about  $1 \times 10^9$  n/cm<sup>2</sup> (this number was not well determined). This system, which was fabricated at LBL as part of a collaborative project with the Carnegie-Mellon group for use at LAMPF with charged particles and consisted of two 1.5cm thick detectors. The neutron irradiation degraded the  $\gamma$ -ray resolution of both detectors from about 2.2 keV to 16 keV at 1332 keV. The system was first connected to a high vacuum pumping station; the cold finger was then removed from the LN<sub>2</sub> dewar and placed in a flask of water that was heated gradually to boiling (91°C at Los Alamos). After a number of hours the procedure was reversed and the detector resolution and capacity as a function of voltage were measured. During the first cycle the detectors were warmed to only room temperature for 60 h and then tested. The detectors were then recycled to 91°C for 60 h, tested, and then cycled again until they had been at 91°C for a total of 300 h. As can be seen in Fig. 11, the resolution was dramatically degraded after the room temperature cycle, but successive treatments gradually restored the resolution to 4 keV after 300 h at 91°C.

Due to the limited resolution of present beams at LAMPF there was no need to fully anneal this system - in fact when the detectors had only 16 keV resolution (prior to any annealing) no effects of radiation damage could be discerned when measuring the high energy charged particles. However, the system was eventually returned to LBL for evaluation and full restoration. After annealing at 150°C for 66 h, both detectors exhibited spectrometer performances and C(V) relationships identical to those obtained originally.

### Conclusions

(1) Significant energy resolution degradation in germanium gamma-ray spectrometers, both lithium-drifted and high purity, occurs after irradiation by between  $10^9$  and  $10^{10}$  n/cm<sup>2</sup> of 5 MeV neutrons

(2) The main finding of this study is that there exists a wide range of damage sensitivities (factor of ten) among high quality germanium spectro-

eters. It is of great interest and importance to elucidate the parameter(s) which is/are responsible. Dislocation density and distribution is an obvious initial and plausible choice. The two detectors which degraded at a distinctly low fluence, 284-1.2 and 287-1.1 had somewhat lower dislocation densities as expressed through etch pit density. Both are from the "head" of each crystal at which position full dislocation patterns may not have fully developed. In fact, a central area of 287-1.1 (as observed on an adjacent slice) was found to be dislocation free, and a dislocation free ring was present in 284-1.2. In contrast, 214-6.0 being further from the head of the ingot and the GE materials are known to have higher EPD. Lithium-drifted detector 40B was fabricated from material with somewhat higher EPD than 43C and does indeed show a slightly greater damage resistance. It is plausible that dislocations represent neutral nucleation sites for neutron-produced vacancies which compete with clustering for the ultimate situation of the vacancies which retain some mobility at LN<sub>2</sub> temperature<sup>12</sup>. Dislocation-free material is known to produce of inferior resolution due to several trapping effects<sup>13</sup>. Specific tests of this hypothesis should be made by comparing detectors from material at the extremes of dislocation densities and distributions. A detector from ingot 284 but much further down in the ingot with a fully developed dislocation pattern will be irradiated.

(3) Changes in the energy resolution take place after irradiation while the detector is held at 77°K. This is not inconsistent with the fact that some vacancy mobility exists at this temperature. Several but not all detectors improved slightly after periods of hours to days following irradiation. Finite but necessarily greatly reduced vacancy mobility might promote recombination during this annealing period, as opposed to agglomeration into trapping clusters. The annealing at LN<sub>2</sub> must therefore cause the spectral degradation resulting from irradiation to exhibit a dependence on neutron dose-rate as well as fluence. Although in most situations, this will not be an important factor, the possibility should be recognized.

(4) Very complete collapse of the energy resolution occurs when anneals at only 200°K, dry ice temperature, are carried out. The acceptor concentration is greatly increased after the dry ice anneal and decreases with further higher temperature anneals. Energy resolution improves somewhat in going from the dry ice anneal to the room temperature anneal.

It is difficult to describe the specific details and dynamics of vacancy clustering and agglomeration in between these two temperatures. However, from a practical viewpoint, it is obvious to instruct that if a germanium spectrometer has been even possibly exposed to fast neutrons, it would be imprudent to recycle the unit to higher temperatures.

(5) A very large portion of recovery is possible from anneals at only 100°C for periods of hours and, further, complete recovery can be achieved at somewhat elevated temperatures, up to 150°C. No solid evidence was found for improved spectrometer performance following damage recovery (compared to initial performance) which may be due in part to the fact that the spectrometers were of high initial performance.

(6) As noted in previous studies, hole trapping predominates as the degrading effect on energy resolution. It should be mentioned here that the

potential use of high purity coaxial detectors offers the possibility of minimizing hole trapping in charge collection if the device is configured with the p<sup>+</sup> contact (Pd) on the coaxial periphery. Thus, the holes make only a short traversal from the outer portions of the detector (where most interactions occur) to the contact of collection. To establish high fields at the periphery one would want to use n-type germanium.

(7) An effect of deep levels increasing the bulk resistance of any undepleted material was observed by means of the pulser introduced through the detector. As this resistivity increases, the undepleted region capacity must be included and the apparent capacity approaches the geometric value constrained to be the series combination of C<sub>u</sub> and C<sub>d</sub>.

(8) An experiment which in the authors' opinion has little prospect of exciting result, should probably be performed for completeness in this area. A detector should be irradiated and annealed to the original performance through several cycles. This situation may arise in practice and it could be that some damage "hardening" may be achieved over several cycles. If this effect occurs it should be studied in a controlled situation.

#### Acknowledgements

We are deeply grateful to Fred Goulding, Keith Jones and Veljko Radeka for helpful discussions and advice. We thank Richard Cordi and Charles Boulin for help in preparation of the detectors and with some of the annealing studies. Ed Reilly was always present to keep the accelerator fit and running. We thank D. E. Alburger for the use of the accelerator. S. Merino and Cas Nawrocki helpfully supplied several neutron producing targets.

#### References

1. J. F. Amann, P. D. Barnes, S. A. Dytman, J. A. Penbrot, A. C. Thompson and R. H. Pehl, submitted to Nucl. Inst. and Meth, (1974).
2. R. W. Whan, Phys. Rev. 160A, 690 (1965).
3. W. L. Hansen, R. H. Pehl, E. J. Rivet and F. S. Goulding, Nucl. Inst. and Meth. 80, 181 (1970).
1. H. W. Kraner, C. Chasman and K. W. Jones, Nucl. Inst. and Meth. 62, 17J (1968).
2. J. Llacer and H. W. Kraner, Nucl. Inst. and Meth. 98, 467 (1972).
3. F. S. Goulding and R. H. Pehl, IEEE Trans, Nuc. Sci. NS-19, No. 1, 91 (1971).
4. P. H. Stelson, A. K. Dickens, S. Raman and R. C. Trammell, Nucl. Inst. and Meth. 98, 481 (1972).
5. N. Bohr, Kg. Danske Videnskab. Selskab, Mat-Fys. Medd. 18, No. 8 (1948).
6. C. Chasman, K. W. Jones and R. A. Ristenen, Nucl. Inst. and Meth. 37, 1 (1965).
7. J. Lindhard, V. Nielsen, M. Scharff and P. V. Thomsen, Kgl. Danske Videnskat, Selskab, Mat-Fys. Medd. 33, No. 10 (1963).
8. C. Chasman, K. W. Jones, H. W. Kraner and W. Brandt, Phys. Rev. Lett. 21, 1430 (1968).
9. J. M. Adams, A. T. G. Ferguson and C. D. McKenzie, A.E.R.E. R 6429 (1970), and W. D. Allen, A.E.R.E. NP/R 1667 (1955).
10. E. E. Haller, W. L. Hansen and F. S. Goulding, IEEE Trans. Nuc. Sci. NS-19, No. 3, 271 (1972).



## Figure Captions

- Fig. 1 Summation of detector response as a function of fast neutron fluence. Detector resolutions less the system contributions are shown with the hours following irradiation in parenthesis. Bias conditions are also noted. The width of each measurement box corresponds to the estimated fractional uncertainty in the fluence measurement, 0.25.
- Fig. 2 Equivalent detector circuit elements for depleted (d) and undepleted (u) regions.
- Fig. 3 C(V) characteristic for detector 284-1.2 at several neutron fluences as measured by the injected pulser method.
- Fig. 4 C(V) characteristic for detector 1098-4 at several neutron fluences as measured by the injected pulser method.
- Fig. 5 C(V) characteristic for detector 287-1.1 at several neutron fluences as measured by the injected pulser method.
- Fig. 6 Oscillograph of preamplifier output waveforms of pulser for detector 284-1.2 at several low biases following irradiation by  $3 \times 10^9$  n/cm<sup>2</sup> of 5.5 MeV neutrons.
- Fig. 7 Oscillograph of preamplifier output waveforms of pulser and <sup>137</sup>Cs spectrum at 100V bias as a function of neutron fluence for detector 1098-4. The amplitude of the pulser is not normalized in these pictures.
- Fig. 8 Oscillograph of amplifier output waveforms of pulser and <sup>137</sup>Cs spectra for detector 287-1.1 showing essentially the initial condition at 900V bias after only  $3 \times 10^9$  n/cm<sup>2</sup> and the resulting decrease in rise times after  $10^{10}$  n/cm<sup>2</sup> of 5.5 MeV fast neutrons.
- Fig. 9(a) The shape of the 1332 keV <sup>60</sup>Co peak at various stages of damage and anneal for detector 214-6.0. The number on each curve refers to the stage listed in the text. No relevance should be attached to the peak positions since the peaks have been displaced and the energy scale varied to clarify the observation of peak shapes.
- 9(b)

Figure Captions(cont'd)

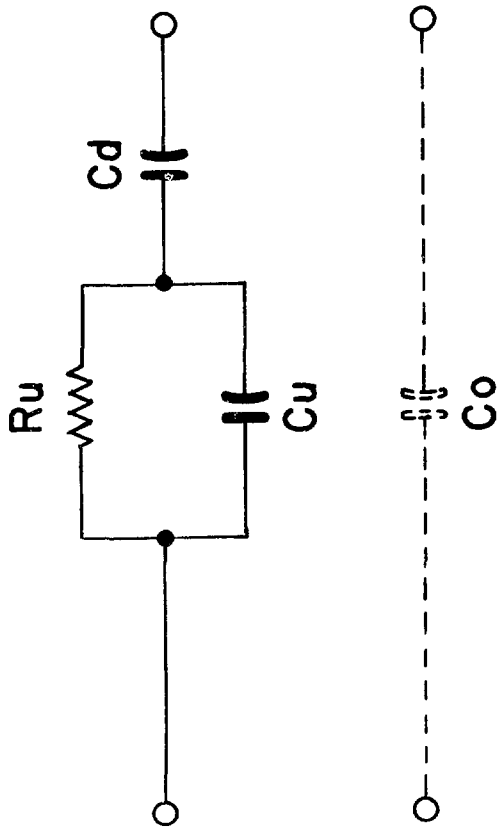
- Fig. 10 The capacity-voltage relationship at various stages for detector 214-6.0. The number on each curve refers to the stage listed in the text.
- Fig. 11 The shape of the 1332 keV  $^{60}\text{Co}$  peak from one 1.5 cm thick germanium detector before, during and after treatment for radiation damage at LAMPF.

**NEUTRON FLUENCE (n/cm<sup>2</sup>)**

DETECTOR	NEUTRON ENERGY (MeV)	INITIAL RESOLUTION (REV)	10 <sup>8</sup>				10 <sup>9</sup>				10 <sup>10</sup>			
			BIAS (V)											
214-6.0	1.4	1.7	500	1.8	2.0	2.1	2.2	2.6	2.8	3.9	4.3			
								2.6 (4)	2.8	3.9 (2)	4.3 (6)	3.5 (2)		
285-1.0	16.4	2.0	2000			2.3	2.7	5.0 (1)	5.0 (1)	9.2	9.3			
								4.8 (1)	4.8 (1)	9.2 (2)	9.3 (2)			
284-1.2	5.5	1.9	600	1.9	1.9 (1)	2.7	3.2	10.6	No PK	No PK	No PK			
								11.3	11.3	11.3 (7)	11.0 (V)			
GE 1	5.5	1.64	650				1.9	2.2	2.8	2.8	4.7			
								2.8 (2)	2.8 (2)	4.7 (4)	4.7 (4)			
GE 2 1098-4	5.5	2.0	1100				2.4	3.3	3.3	5.3	7.1	2.3		
								4.3 (3)	4.3 (3)	5.3 (1)	7.1 (1)	2.3 (1)	2.3	
287-1.1	5.5	1.8	650					7.8	No PK	No PK	No PK			
								7.8 (1)	7.8 (1)	11.2 (10)	11.0 (V)			
GE 3 1098-2 (6 mm)	5.5	1.7	900			1.6	1.7	2.0	1.6	1.6	1.9			
								2.0	1.6	1.6	1.9 (2)	2.7 (3)	3.0 (1)	
Ge (Li) 40B	5.5	1.8	1900				1.9	1.8	2.3	3.1	3.0			
								1.8	2.3	3.1	3.0			
Ge (Li) 43C	5.5	2.1	2600				2.3	3.1	4.2	4.6				
								2.3 (1)	3.1	4.2	4.6			

Notes: ① Background is estimated error at flux determination.  
 ② Numbers in parentheses in lower portion of biases indicate bias post irradiation;  $\sigma$  is  $\pm$  error;  $\sigma$  is  $\pm$  error;  $\sigma$  is  $\pm$  error.

FIGURE 1



$$C_o = \frac{C_d C_u}{C_d + C_u}$$

FIGURE 2

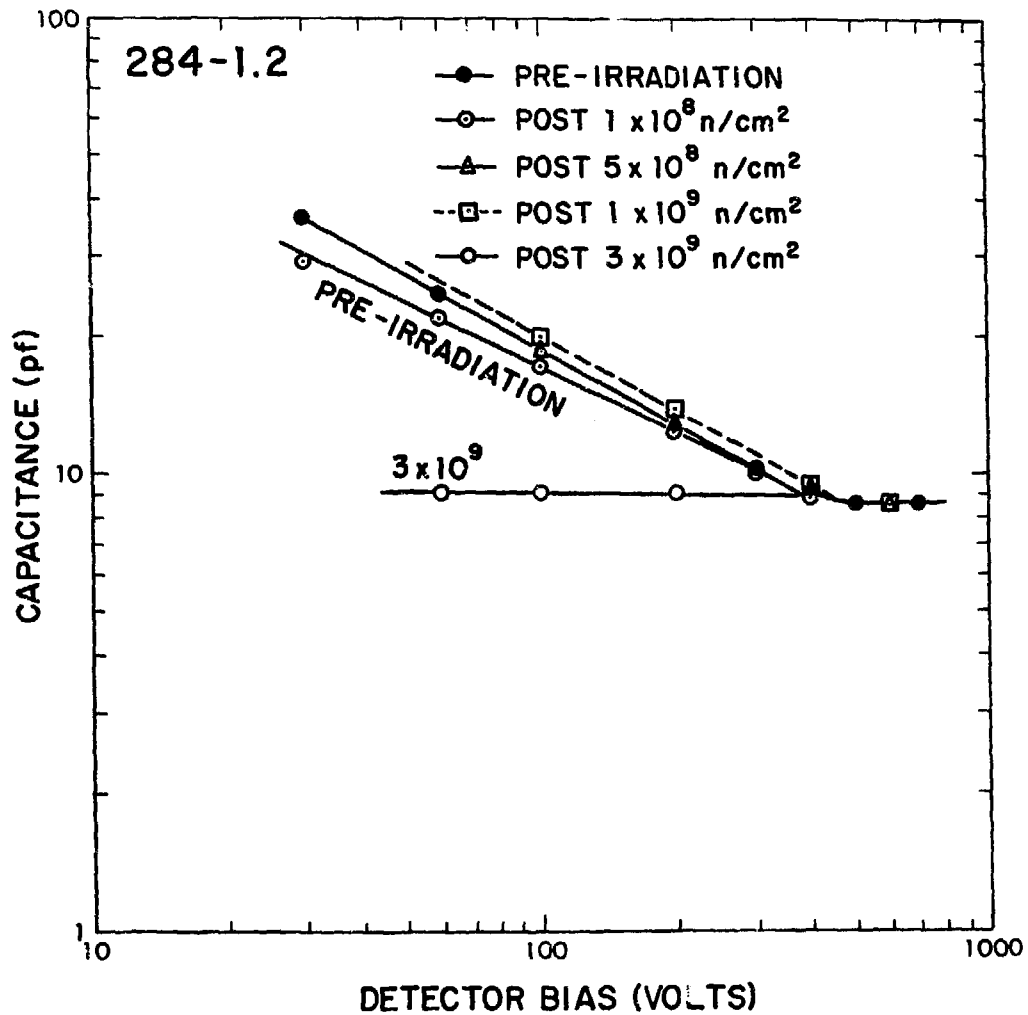


FIGURE 3

FIGURE 4

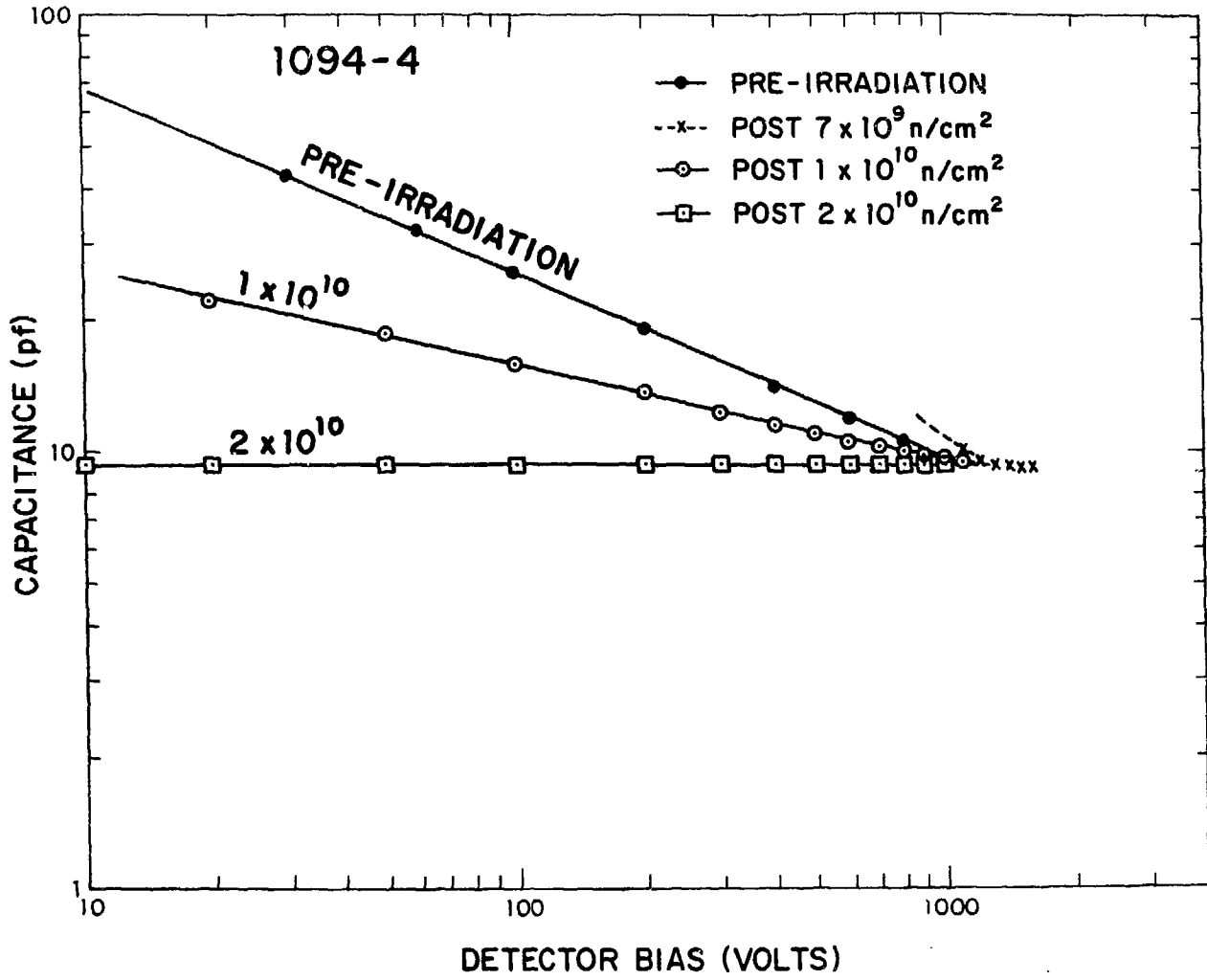
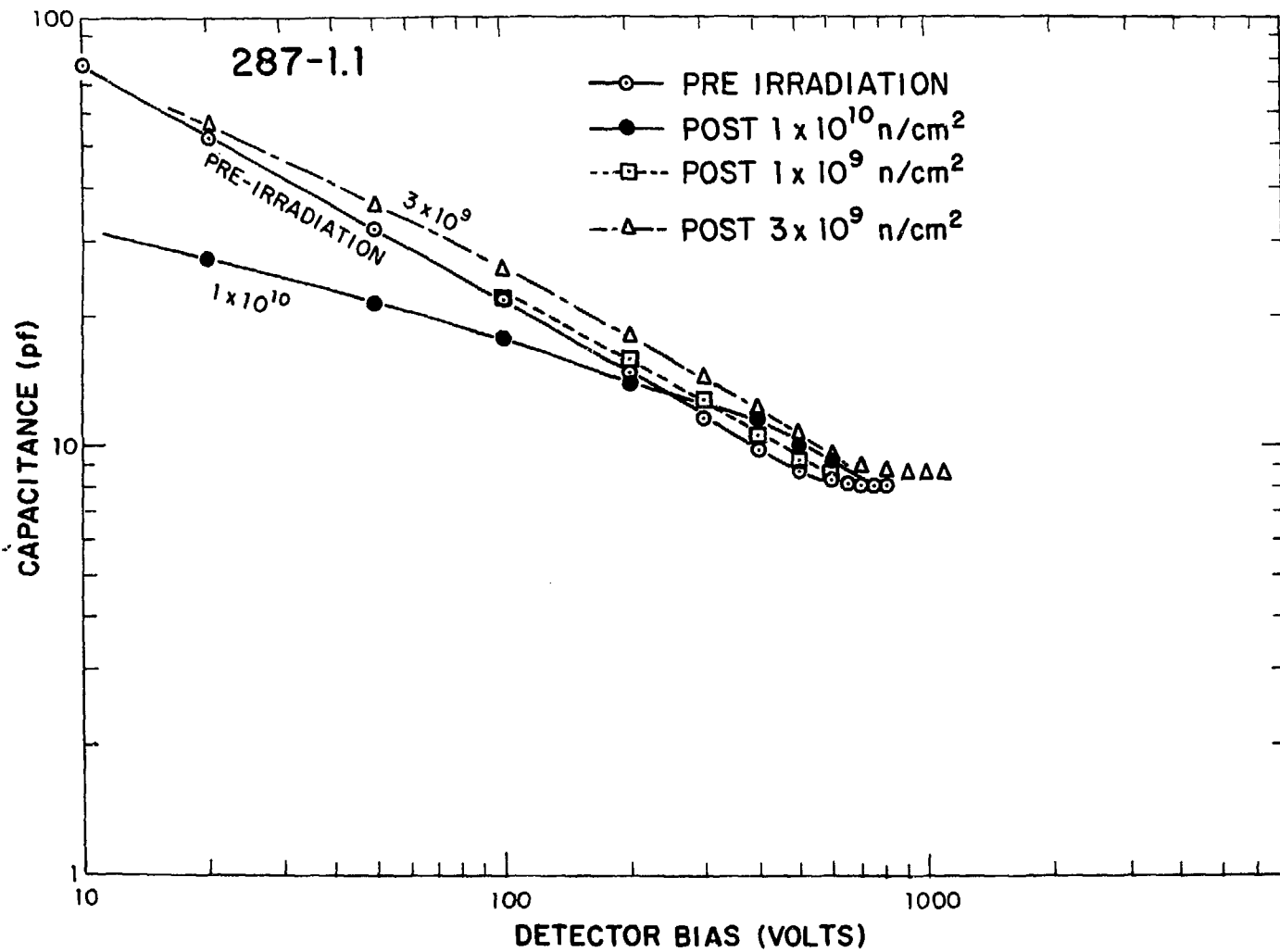


FIGURE 5



284-1.2  
POST  $3 \times 10^9 \text{ n/cm}^2$

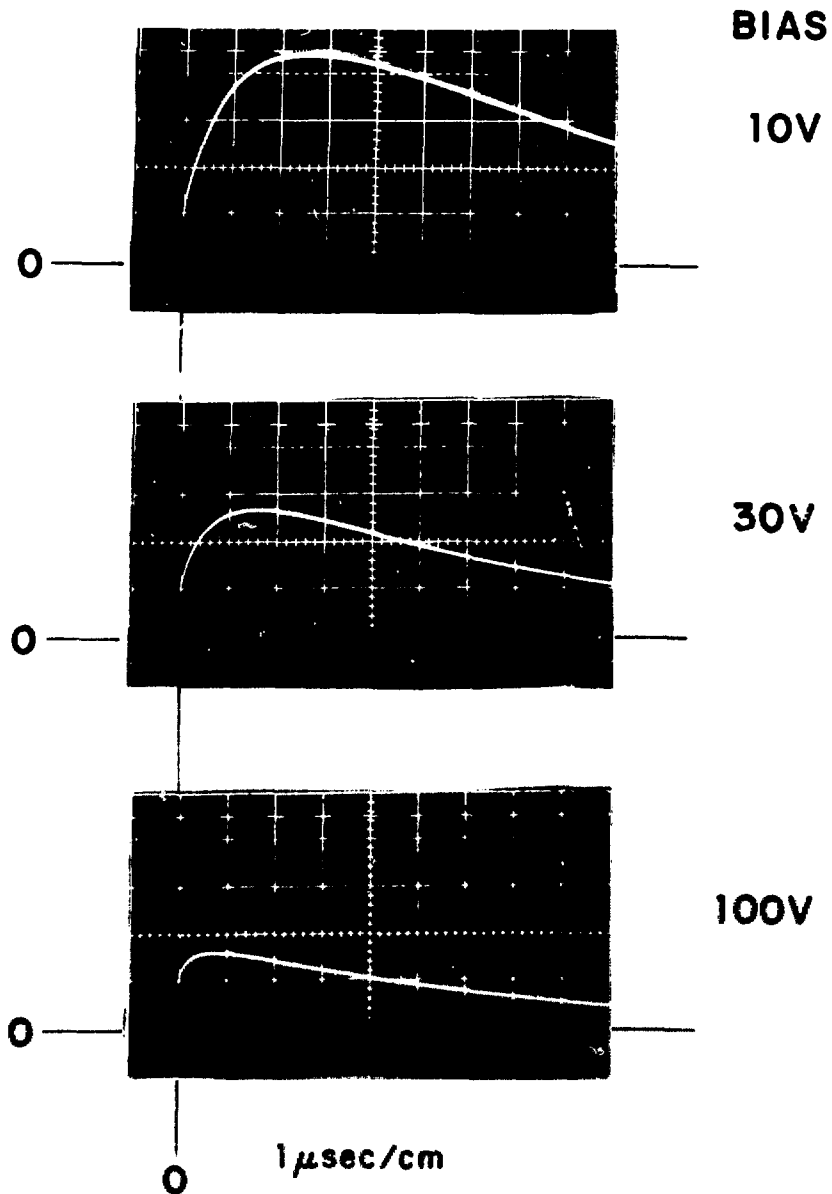
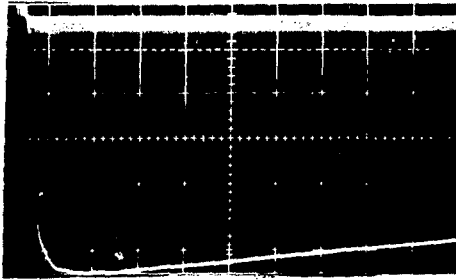


FIGURE 6

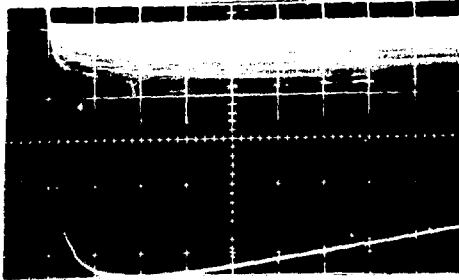


1098-4



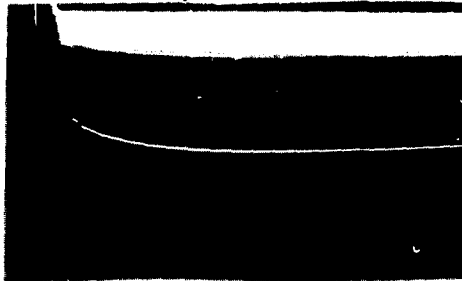
0.5  $\mu$ sec/cm

100V  
POST  
 $3 \times 10^9$



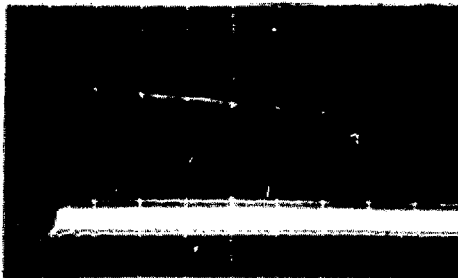
1.0  $\mu$ sec/cm

100V  
POST  
 $7 \times 10^9$



1.0  $\mu$ sec/cm

100V  
POST  
 $1 \times 10^{10}$

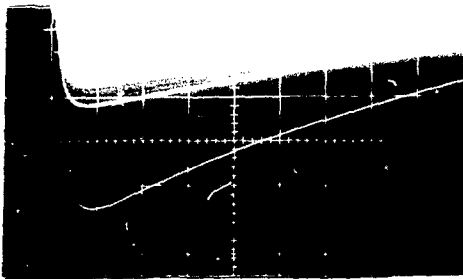


1.0  $\mu$ sec/cm

100V  
18hrs POST  
 $2 \times 10^{10}$   
C(V) NOW FLAT

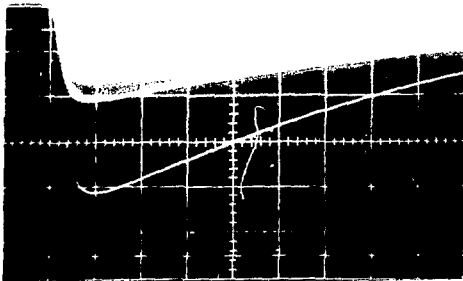
FIGURE 7

287-1.1



900V

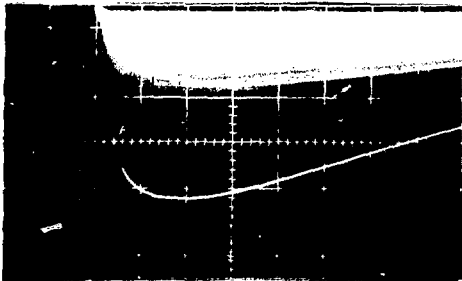
$3 \times 10^9$



200V

16hrs POST

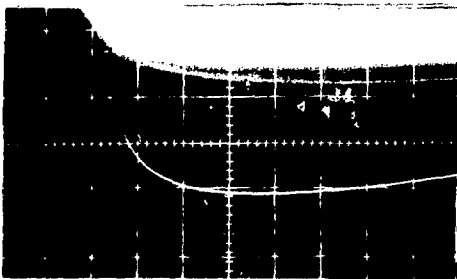
$3 \times 10^9$  n/cm<sup>2</sup>



200V

1hr POST

$1 \times 10^{10}$  n/cm<sup>2</sup>



200V

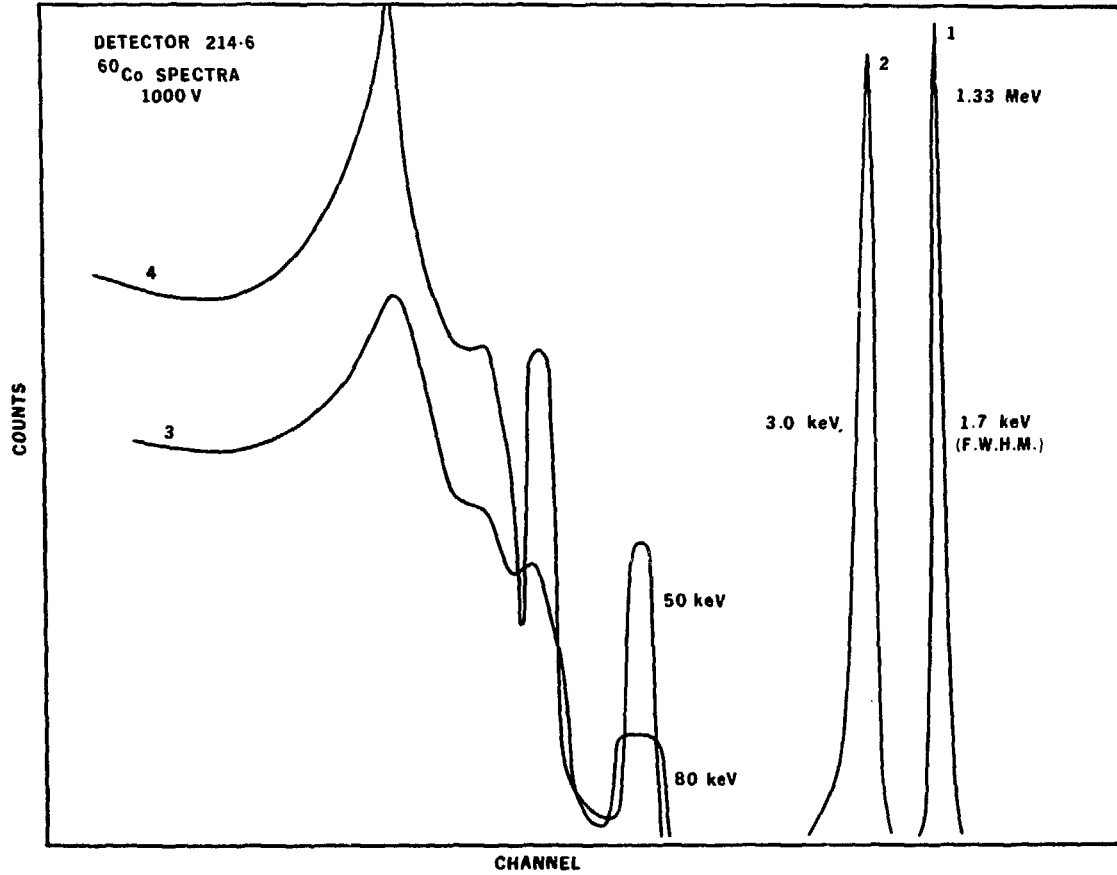
17hrs POST

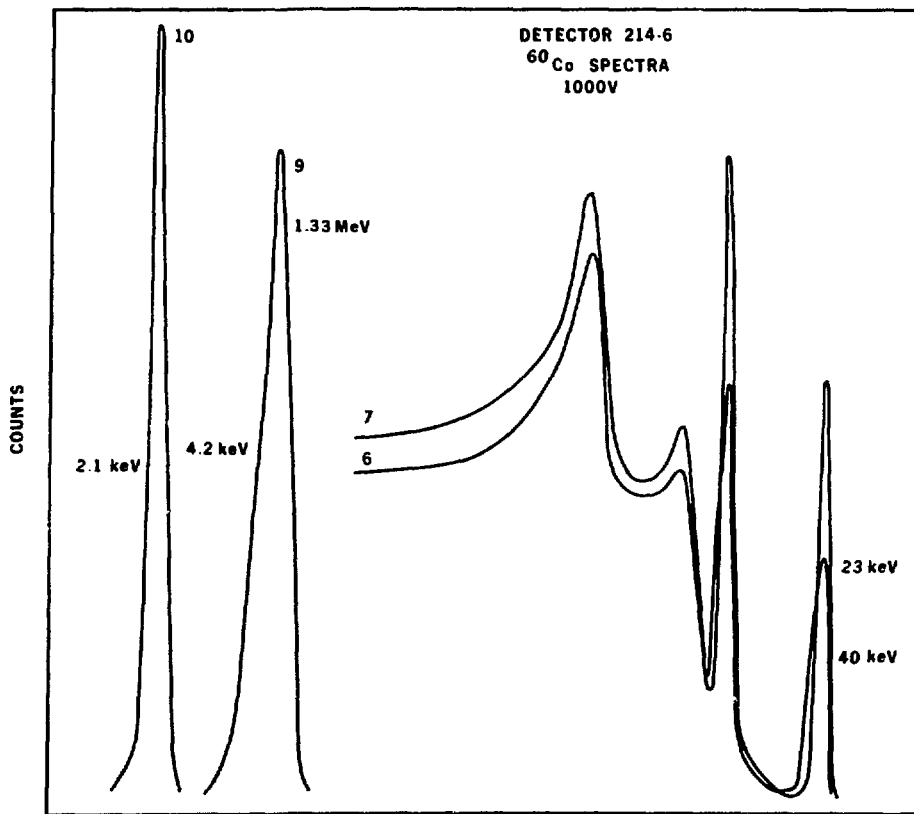
$1 \times 10^{10}$  n/cm<sup>2</sup>

1  $\mu$ sec/cm

FIGURE 8

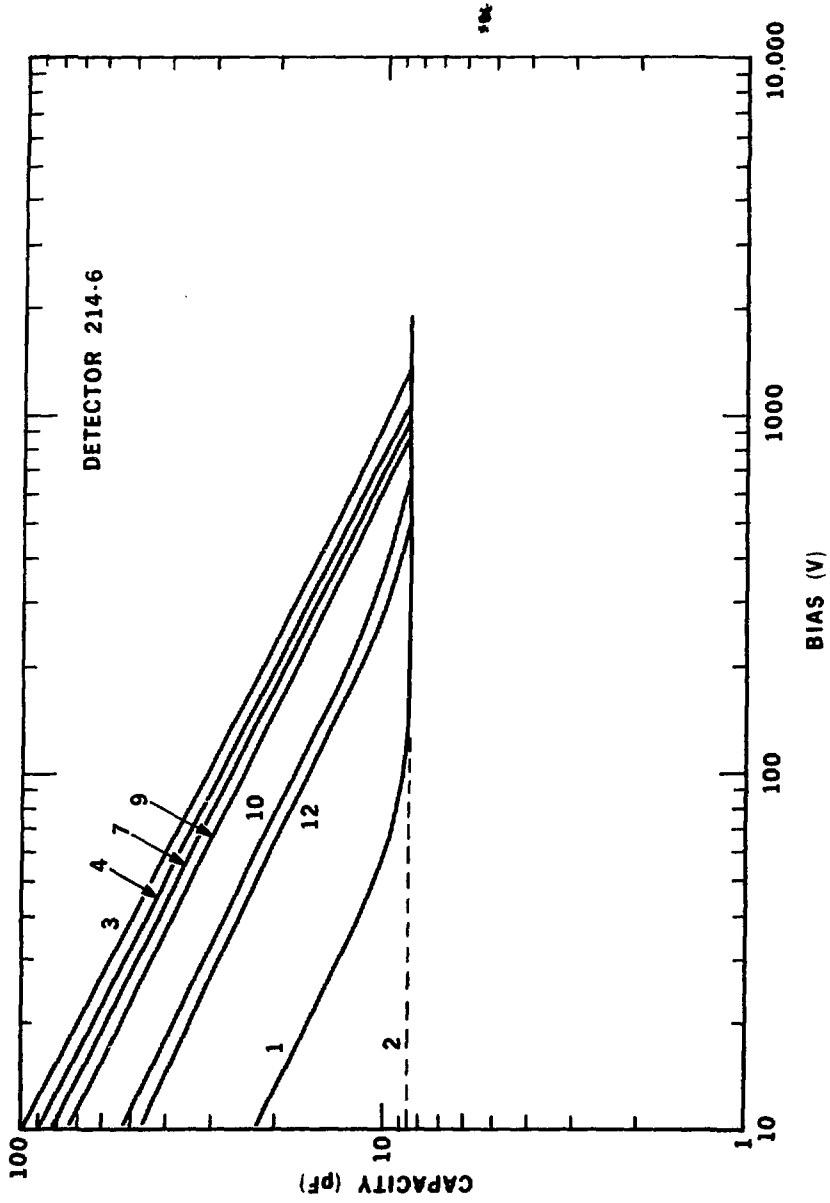
FIGURE 9 (a)





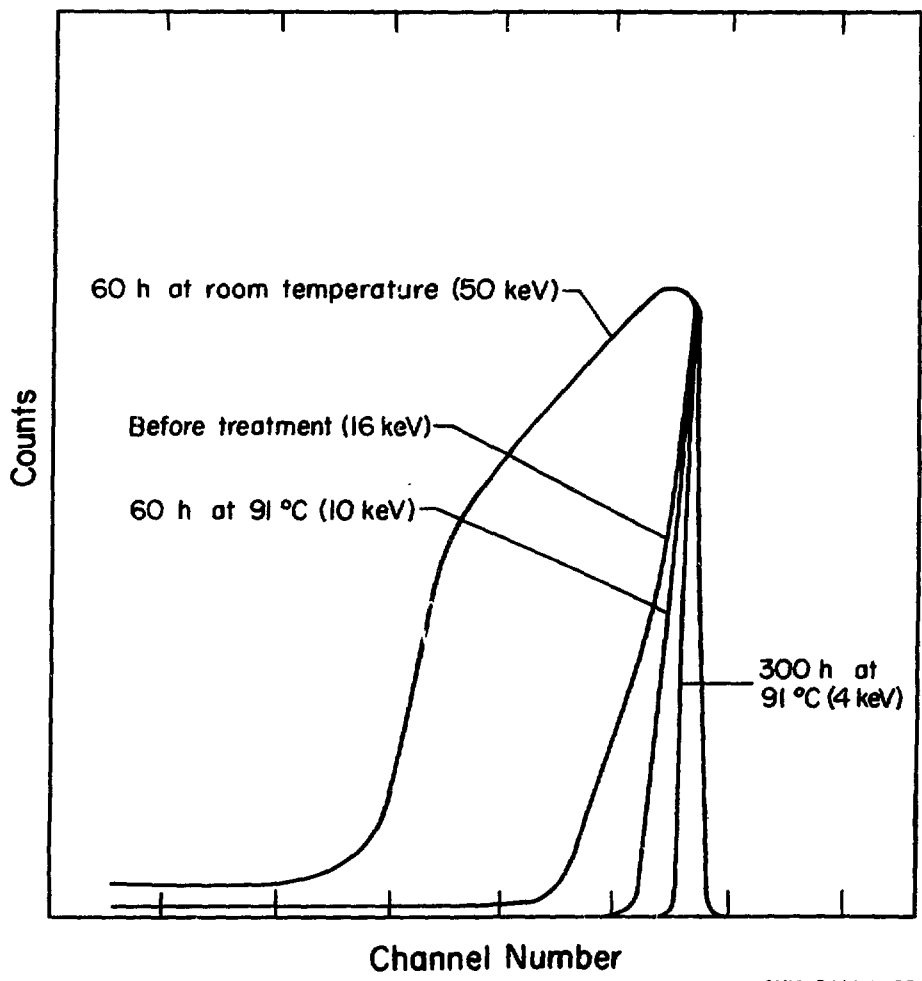
NBL 7411 8635

FIGURE 9(b)



800

FIGURE 10



NBL 7411-8022

FIGURE 11